ARTICLE
Journal of Cellular Biochemistry 113:2607–2621 (2012)

Journal of Cellular Biochemistry

Perinuclear Positioning of the Inactive Human Cystic Fibrosis Gene Depends on CTCF, A-Type Lamins and an Active Histone Deacetylase

Joscha S. Muck,[1] Karthikeyan Kandasamy,[1] Andreas Englmann,[2] Martin Günther,[1] and Daniele Zink[1*]

[1]*Institute of Bioengineering and Nanotechnology (IBN), Department of Cell and Tissue Engineering, 31 Biopolis Way, The Nanos, Singapore 138669*

[2]*Ludwig-Maximilians-Universität (LMU) München, Biozentrum, Department Biologie II, Grosshadernerstr. 2, 82152 Planegg-Martinsried, Germany*

ABSTRACT

The nuclear positioning of mammalian genes often correlates with their functional state. For instance, the human cystic fibrosis transmembrane conductance regulator (CFTR) gene associates with the nuclear periphery in its inactive state, but occupies interior positions when active. It is not understood how nuclear gene positioning is determined. Here, we investigated trichostatin A (TSA)-induced repositioning of CFTR in order to address molecular mechanisms controlling gene positioning. Treatment with the histone deacetylase (HDAC) inhibitor TSA induced increased histone acetylation and CFTR repositioning towards the interior within 20 min. When CFTR localized in the nuclear interior (either after TSA treatment or when the gene was active) consistent histone H3 hyperacetylation was observed at a CTCF site close to the CFTR promoter. Knockdown experiments revealed that CTCF was essential for perinuclear CFTR positioning and both, CTCF knockdown as well as TSA treatment had similar and CFTR-specific effects on radial positioning. Furthermore, knockdown experiments revealed that also A-type lamins were required for the perinuclear positioning of CFTR. Together, the results showed that CTCF, A-type lamins and an active HDAC were essential for perinuclear positioning of CFTR and these components acted on a CTCF site adjacent to the CFTR promoter. The results are consistent with the idea that CTCF bound close to the CFTR promoter, A-type lamins and an active HDAC form a complex at the nuclear periphery, which becomes disrupted upon inhibition of the HDAC, leading to the observed release of CFTR. J. Cell. Biochem. 113: 2607–2621, 2012.

KEY WORDS: NUCLEAR ARCHITECTURE; GENE POSITIONING; CYSTIC FIBROSIS TRANSMEMBRANE CONDUCTANCE REGULATOR; HISTONE MODIFICATIONS; HISTONE ACETYLATION

Transcription is regulated at multiple levels. *cis*-regulatory factors play an important role as well as modifications of local chromatin structure. Chromatin modifying enzymes are often targeted by *cis*-regulatory factors to specific gene loci and in this way changes at both regulatory levels can be coordinated.

Also the higher-order organization of chromatin in the cell nucleus might contribute to gene regulation and the nuclear positioning of gene loci often correlates with their functional status [Fedorova and Zink, 2008; Ferrai et al., 2010]. Typical for mammalian nuclei is a radial organization with inactive loci occupying more peripheral positions [Croft et al., 1999; Sadoni et al., 1999; Cremer et al., 2001; Tanabe et al., 2002; Fedorova and Zink, 2009]. It is not well understood how higher-order chromatin organization is regulated and how it is coordinated and integrated with other levels of transcriptional regulation.

Joscha S. Muck and Karthikeyan Kandasamy contributed equally to the work.

Additional supporting information may be found in the online version of this article.

Grant sponsor: Institute of Bioengineering and Nanotechnology (Biomedical Research Council, Agency for Science, Technology and Research, Singapore).

Andreas Englmann's present address is Sabel Realschule München, Schwanthalerstraße 51–57, 80336 München, Germany.

*Correspondence to: Daniele Zink, Institute of Bioengineering and Nanotechnology (IBN), Department of Cell and Tissue Engineering, 31 Biopolis Way, The Nanos, Singapore 138669. E-mail: dzink@ibn.a-star.edu.sg

Manuscript Received: 7 March 2012; Manuscript Accepted: 8 March 2012

Accepted manuscript online in Wiley Online Library (wileyonlinelibrary.com): 15 March 2012

DOI 10.1002/jcb.24136 • © 2012 Wiley Periodicals, Inc.

One factor, which has been shown to play an important role in higher-order chromatin organization, is the CCCTC-binding factor CTCF. This factor, which was originally described as a transcriptional repressor, appears to be able to link discrete domains on the same or different chromosomes [Ling et al., 2006; Splinter et al., 2006] and seems to be crucial for the organization of chromatin loops [Phillips and Corces, 2009; Zlatanova and Caiafa, 2009a]. CTCF-dependent insulator and barrier functions have been demonstrated [Bell et al., 1999; Hark et al., 2000; Witcher and Emerson, 2009] and it has been shown that CTCF tethers an insulator to the nucleolus [Yusufzai et al., 2004]. Thus, CTCF also appears to play a role in the positioning of loci at specific nuclear regions. This view is supported by the recent findings that perinuclear positioning and insulator functions of the human D4Z4 subtelomeric repeat depend on CTCF, as well as on A-type lamins [Ottaviani et al., 2009ab]. CTCF and lamin A/C have been copurified in soluble extracts from HeLa cells over-expressing CTCF [Yusufzai et al., 2004], suggesting functional interactions between these proteins.

In addition to the functions described here CTCF appears to be involved in the regulation of various other processes. It appears that posttranslational modifications and interactions with specific protein binding partners and functional complexes specify CTCF functions at a particular binding site [Phillips and Corces, 2009; Zlatanova and Caiafa, 2009b; Ohlsson et al., 2010].

In addition to CTCF, local chromatin structure and the patterns of histone modifications might play a role in determining gene positioning. It has been observed in a murine genetic model of human diabetes that hepatocyte nuclear factor (HNF) 1α-dependent local chromatin modifications are linked to radial gene positioning [Luco et al., 2008]. This study addressed histone H3 methylation at lysine residues 4 and 27, but it should be noted that HNf1α also impacts the patterns of histone acetylation [Parrizas et al., 2001; Soutoglou et al., 2001].

Relationships between the patterns of histone acetylation and gene positioning have been observed in various model systems [Sadoni et al., 1999; Schübeler et al., 2000; Zink, 2006; Fedorova and Zink, 2008; Strasak et al., 2009]. The strongest evidence for a functional link comes from the observation that treatment with the histone deacetylase (HDAC) inhibitor trichostatin A (TSA) drives gene loci from the nuclear periphery into the interior in human [Zink et al., 2004] and Drosophila [Pickersgill et al., 2006] cells. In human nuclei TSA treatment leads to repositioning of the inactive cystic fibrosis transmembrane conductance regulator (CFTR) gene from the periphery into the interior [Zink et al., 2004]. Normally CFTR only resides in the nuclear interior when it is active. TSA treatment does not lead to transcriptional activation of CFTR [Zink et al., 2004; Englmann et al., 2005].

Here, we used this model system to identify molecular components determining radial gene positioning. We identified three essential components of a mechanism that controlled perinuclear positioning of the inactive CFTR gene: CTCF, lamin A/C and an active HDAC. These components acted on a CTCF site adjacent to the CFTR promoter. The results are consistent with the idea that CTCF bound close to the CFTR promoter, A-type lamins and an active HDAC form a complex at the nuclear periphery, which becomes disrupted upon inhibition of the HDAC, leading to the observed release of CFTR.

MATERIALS AND METHODS

CELL CULTURE

HeLa S3, HEK 293, and Calu-3 cells were obtained from the American Type Culture Collection (Manassas, VA). HeLa cells were cultivated with DMEM containing 10% fetal bovine serum. The other cell types were cultivated as recommended. TSA (Sigma-Aldrich, Singapore) was used at a concentration of 10 ng/ml.

FISH AND EROSION ANALYSIS

FISH experiments (CF1 probe for CFTR) and two-dimensional (2D) erosion analyses were performed as described [Zink et al., 2004]. Three-dimensional (3D) erosion analyses were performed as outlined previously [Sadoni et al., 2008].

IMMUNOBLOTTING AND IMMUNOSTAINING

The immunoblotting procedure was performed as described [Zhang et al., 2009]. For some experiments the following protocol was used: about 1×10^6 cells were lysed in 75°C warm lysis buffer (1% sodium dodecyl sulfate (SDS), 50 mM Tris–HCl, pH 8.0). The lysate was sonicated for 1 min and the absorption was measured at 230, 260, and 280 nm. Probes analyzed in parallel were adjusted to a similar optical density using 4× LDS NuPAGE sample buffer (Invitrogen, Singapore). NuPAGE 8–12% Bis–Tris gradient gels (Invitrogen) were used as recommended. Transfer to polyvinylidene fluoride (PVDF) membranes was performed with the iBlot system (Invitrogen). PVDF membranes were blocked for 3 h with RIPA buffer (150 mM NaCl, 0.25% deoxycholate, 1% Triton X-100, 50 mM Tris–HCl, pH 8.0) containing 5% bovine serum albumin (BSA). Incubations with the primary and secondary antibodies were performed over night at 4°C. Between these incubations the membranes were washed 3×5 min with RIPA buffer. After the incubation with the secondary antibody the membranes were washed 2×10 min with RIPA buffer and once with RIPA buffer containing 0.03% SDS and were rinsed twice in deionized water. Detection was performed using chemiluminescence (SuperSignal West Femto, Thermo Scientific, Waltham) and a gel documentation device (ChemiDoc XRS, Biorad, Hercules). Densitometry was performed using QuantityOne 4.6.7. software. Immunostaining was performed as described [Sadoni et al., 1999].

ANTIBODIES

A rabbit anti-CTCF antibody (2899) and an antibody against acetylated lysines (Ac-K-103) were obtained from Cell Signaling (Danvers, MA). The following antibodies were purchased from Abcam (Cambridge, UK): mouse anti-β-actin (ab 8224), rabbit anti-H3K4me3 (ab 1012), rabbit anti-histone H3 K9me3 (ab 8898), rabbit anti-histone H3 (ab 1791). The following antibodies raised in rabbits were purchased from Millipore (Billerica, MA): anti-histone H3 K27me3 (07-449), anti-acetyl histone H3 (06-599), and anti-acetyl histone H4 (6-866). The anti-lamin A/C antibody (mouse, monoclonal) was obtained from Santa Cruz Biotechnology (Santa Cruz, CA, USA). Secondary anti-mouse and anti-rabbit antibodies either conjugated to enzymes (horse radish peroxidase or alkaline

phosphatase) or fluorochromes were obtained from Promega (Madison, WI), Santa Cruz Biotechnology, Invitrogen, and Abcam.

IMMUNOPRECIPITATION (IP) AND ChIP

For IP of acetylated proteins, protein A Dynabeads (Invitrogen) were used and manufacturer's instructions (http://products.invitrogen.com/ivgn/product/10002D) were followed. For cross-linking chromatin immunoprecipitation (X-ChIP) with the CTCF antibody the Millipore protocol (http://www.millipore.com/userguides/tech1/mcproto407) was used. For histone X-ChIP the Abcam protocol (http://www.abcam.com/index.html?pageconfig=resource&rid=11698) was applied with the following modifications: cross-linking was performed with 1.7% formaldehyde for 6 min. Cells were lysed in RIPA buffer (150 mM NaCl, 0.25% deoxycholate, 1% Triton X-100, 50 mM Tris–HCl, pH 8.0) with 2 mM EDTA and freshly added protease inhibitor set (complete mini, Roche, Basel, Switzerland). Chromatin was sonicated with a HTU Soni 130 ultrasonic homogenizer (G. Heinemann, Schwabisch Gmund, Germany). Gel electrophoresis and densitometric analysis revealed that ~60% of the fragments had a length of ~200 bp (~80% < 1,000 bp). To reverse cross-links protein A/G Dynabeads (Invitrogen) were resuspended in 100 µl PBS with 10 µl 5 M NaCl-solution and incubated for 6 h (or overnight) at 65°C. DNA was purified using the Qiaquick PCR Purification kit (Qiagen, Hilden, Germany). At least three independent ChIP experiments were performed for each condition (untreated or TSA-treated), antibody and cell type. Amplification of the ChIP-DNA was performed with the GenomePlex Complete WGA Kit (WGA2) according to the manufacturer's instructions (Sigma-Aldrich). For labeling the Label IT µArray Labeling Kit Cy3/Cy5 (Mirus Bio LLC, Madison, WI) was applied.

DNA MICROARRAYS

The DNA microarrays were purchased from Agilent Technologies (Santa Clara, CA) and were designed with the software eArray (https://earray.chem.agilent.com/erray/). Validated isothermal probes within base pairs 116,200,000–117,400,000 (human genome assembly hg18) of human chromosome 7 were selected and a set of 9,968 individual probes was obtained. Each chip contained four identical sectors and each sector contained four identical individual probe sets. In addition, each sector contained the (−)3xSLv1 control set of probes and other controls. Hybridization was performed according to the manufacturer's instructions using the Stabilization and Drying kit (Agilent Technologies). Four sectors were hybridized for each condition (untreated or TSA-treated) and histone isoform (H4ac and H3ac) in case of HeLa cells using the DNA derived from the independent ChIP experiments. Two sectors were hybridized for each condition and histone isoform in case of Calu-3 cells (the DNA derived from two of the three independent ChIP experiments was pooled and hybridized to one sector; the other sector was hybridized with DNA derived from the third independent ChIP experiment). DNA microarrays were scanned with an Axon Genepix 4200AL Scanner (Molecular Devices, Sunnyvale, CA) using the software Genepix Pro 6.0. The UCSC (University of California, Santa Cruz, CA, USA) Genome Browser (http://genome.ucsc.edu/) was used for displaying the results and for comparisons with ENCODE data. The results from all sectors belonging to the same experimental condition (cell type, treatment, histone isoform) were averaged and the mean values obtained for each probe on the DNA chip are displayed in Figure 3.

qPCR

For validation of DNA-chip data qPCR primers were generated using the online tool primerblast (www.ncbi.nlm.nih.gov/tools/primer-blast/) and the DNA sequence of the DNA-chip probe as well as 70 bp flanking regions. From the suggested primer pairs those closest to the DNA-chip probe were chosen. Primerblast was also applied to generate primer pairs for the analysis of CTCF binding sites using the positions of the CTCF binding sites mapped by the ENCODE project. The exact positions and DNA sequences of the primer pairs will be provided upon request. All primer pairs selected generated in qPCR reactions a single product and showed the same amplification efficiency. qPCR was performed with the KAPA SybrGreen Universal kit and the KAPA SybrFast kit (Kapa Biosystems, Woburn, MA) using the 7500 Fast Real Time PCR System (Applied Biosystems, Foster City, CA). In each case ChIP-DNA from three independent ChIP experiments (10 ng ChIP-DNA per reaction) was analyzed with three technical replicates per ChIP experiment and primer pair. C_t values were determined with the 7500 software (2.0.3, Applied Biosystems).

RNA INTERFERENCE (RNAi)

RNAi was performed with unspecific (Block-iT, Invitrogen or ON-TARGETplus NON-targeting siRNA #1, Dharmacon RNAi Technologies, Lafayette, CO) or specific siRNA. For CTCF the following specific siRNA was used: CTCF Stealth Select RNAi^{TM} siRNA, mix of three oligos: HSS116455, HSS116456, HSS 173820 (Invitrogen). The siRNA specific for lamin A/C was obtained from Applied Biosystems (lamin A/C Silencer Select siRNA, AM16810 s8221) and from Qiagen. For knockdown of SIN3A the specific ON-TARGETplus SMART pool siRNA oligos were used. Knockdown of GGT was performed with Silencer select pre-designed siRNA from Invitrogen. The experiments were performed with serum-free Opti-MEM medium (Invitrogen) and RNAiMAX reagent (Invitrogen). After 6 h of incubating the cells with the complexed siRNA the Opti-MEM medium was replaced by normal serum-containing cell culture medium. After 3 days the treated cells were split in order to obtain samples suitable for parallel processing (immunoblotting, immunostaining, FISH). These procedures were performed on the following day.

STATISTICS

ChIP–chip data were analyzed using the Microsoft Excel add-in Macro ChIPOTle [Buck et al., 2005]. The following parameters were selected: sliding window of 1,000 bp, step size of 250 bp, normal distribution and a *P*-value of 0.001. In case of immunoblotting, FISH (comparison of FISH signals in the outermost shell) and ChIP–qPCR data (C_t values) quantile–quantile (Q-Q) plots were generated as described (http://lieblab.bio.unc.edu/ChIPOTle/ChIPOTle_Readme_v1.0.pdf) in order to determine whether the data display a normal distribution. Log_e-transformed data were used in case of immunoblotting results. Q-Q plots were analyzed by linear regression analysis and in all cases a normal distribution was observed. As the

results suggested variance heterogeneity the Welch's *t*-test was selected for the analysis of the immunoblotting, FISH and ChIP–qPCR results.

RESULTS

KINETICS OF TSA-INDUCED HISTONE HYPERACETYLATION AND CFTR REPOSITIONING

In order to investigate whether changes in the patterns of histone acetylation could cause CFTR (NM_000492.3, gene ID 1080) repositioning we investigated first the temporal relationships between TSA-induced histone hyperacetylation and CFTR repositioning. The kinetics of TSA-induced global histone hyperacetylation were investigated by treating HeLa cells for 20, 40, 60, 80, and 100 min with 10 ng/ml of TSA. Acetylated histones H3 and H4 (H3ac and H4ac) were detected in cell lysates by immunoblotting and densitometric analysis (Fig. 1). The data confirmed that TSA treatment increased global histone hyperacetylation. Significant increases in the amounts of H3ac ($P < 0.001$) and H4ac ($P < 0.05$) could be detected after 20 min. The amounts of H3ac did not further increase significantly at later time points. The amounts of H4ac showed additional significant increases at 40 min (compared to 20 min; $P < 0.05$) and 80 min (compared to 40 min; $P < 0.05$).

Next, we analyzed the kinetics of TSA-induced repositioning of CFTR. For this purpose HeLa cells were treated for time periods of 10, 20, 30, 40, 50, 60, and 600 min with TSA. The 600 min time point served as positive control as it had been shown before the CFTR has relocalized into the nuclear interior after this time period [Zink et al., 2004]. CFTR positioning was determined by fluorescence in situ hybridization (FISH) followed by 2D erosion analysis, which has been demonstrated repeatedly to be an accurate and reliable method for determining the nuclear positioning of CFTR and adjacent genes [Zink et al., 2004; Sadoni et al., 2008].

Figure 2 shows that more than 40% of CFTR-specific FISH signals were found in the outermost nuclear zone in untreated cells. This distribution was typically observed when CFTR was associated with the nuclear periphery and localized in the perinuclear heterochromatin [Zink et al., 2004; Sadoni et al., 2008]. The numbers of FISH signals in the outermost zone decreased significantly after 20 min of TSA treatment ($P < 0.05$) and dropped below 40%. This distribution was typically observed when CFTR was associated with euchromatin localizing at more interior nuclear positions [Zink et al., 2004; Sadoni et al., 2008] (the nuclear interior is defined here as the nuclear space interior from the perinuclear heterochromatin). Between 40 and 60 min an additional significant change in the positioning of CFTR was observed ($P < 0.05$). After 60 min no further significant changes in the positioning of CFTR occurred (compare 60 and 600 min; we also tested in addition 75, 120, 270, and 480 min and observed no further significant changes (data not shown)). Repositioning of CFTR after 20 min of TSA treatment was

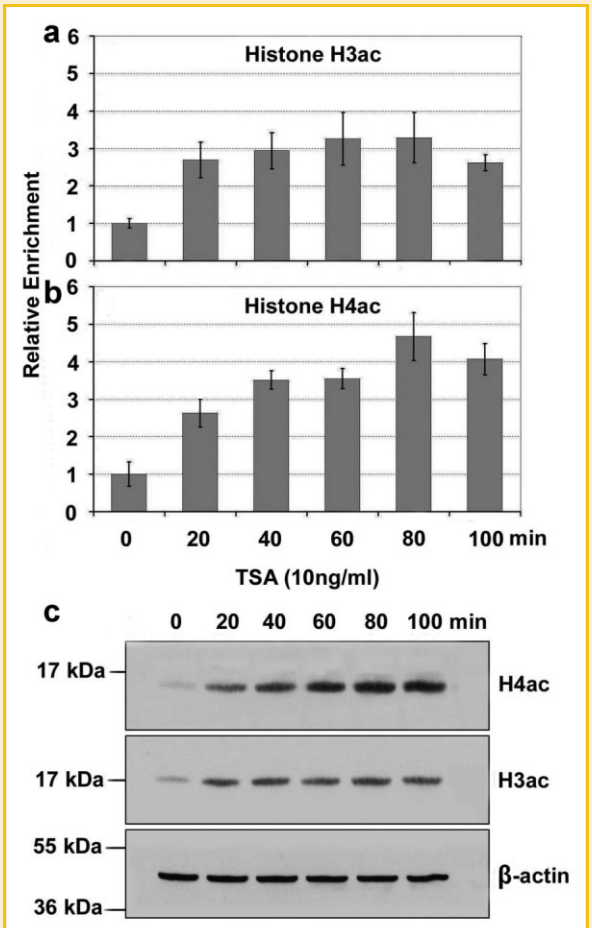

Fig. 1. Increase in the levels of H3ac and H4ac during TSA treatment. HeLa cells were treated with TSA (10 ng/ml) for the time periods indicated. Cell lysates were analyzed by immunoblotting and densitometric analysis. The data in panels a and b show the mean values ± standard error of the mean (SEM, n = 3–8). The mean values from untreated cells (0 min) were set to 1. Panel c shows the results of an immunoblotting experiment. The positions of the bands of the size marker and the sizes of the respective peptides (kilodalton, kDa) are indicated on the left. β-actin was used as loading control.

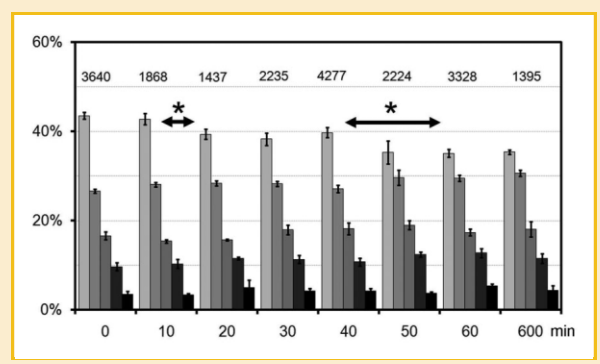

Fig. 2. Changes in the positioning of CFTR during TSA treatment. HeLa cells were treated for the indicated time periods with TSA. CFTR positioning was determined by FISH and 2D erosion analysis. Nuclei were subdivided into five concentric shells. For each time point, the five bars indicate the percentages of CFTR-specific FISH signals in the different shells (mean ± SEM; light gray: peripheral shell, black: center). At least three replicates were analyzed in each case and the numbers above the diagrams indicate the numbers of FISH signals evaluated. Asterisks denote significant ($P < 0.05$) changes in the numbers of FISH signals in the outermost shell during the time interval indicated by the arrow.

also observed in primary human epithelial cells (primary human renal proximal tubule cells; Supplementary Data, Fig. S1a). Thus, rapid TSA-induced repositioning of CFTR is not an aberrant feature of transformed cells. Together, the data showed a temporal coincidence between CFTR repositioning and histone hyperacetylation and in both cases the first significant changes already occurred after 20 min.

For the correct interpretation of the results of the erosion analysis it should be noted that the erosion analysis with 2D image data, as performed here, reliably indicates repositioning of gene loci from the nuclear periphery to the nuclear interior, as demonstrated before by comparison of 2D and 3D data sets [Zink et al., 2004; Sadoni et al., 2008]. However, the 2D erosion analysis data do not reveal the total numbers of gene loci localizing at a particular nuclear region and relatively small changes in percentages observed in the 2D erosion analysis reflect major rearrangements in nuclear space. Thus, we found in agreement with our previous results [Zink et al., 2004; Sadoni et al., 2008], that in total ~80–90% of the gene loci localize in the outermost shell, as revealed by 3D erosion analysis, when ~45% of gene loci are found in this shell in the 2D erosion analysis (Figs. S2 and S9). Also, when the numbers of gene loci in the outermost shell drop from ~45% to ~40% or less in the 2D erosion analysis this reflects a drop in total numbers of gene loci by at least 20–30%, as demonstrated by 3D erosion analyses [Figs. S2 and S9, see also Zink et al., 2004; Sadoni et al., 2008].

THE PATTERNS OF H3ac AND H4ac IN A 1.2 MEGA BASE PAIRS (Mb) REGION ON HUMAN CHROMOSOME 7

The following experiments were designed in order to find out which changes of histone acetylation patterns occurred at the CFTR locus within 20 min of TSA treatment and which genomic sites displaying such changes might be involved in the regulation of CFTR positioning. In order to address these questions we analyzed the patterns of histone H3 and H4 acetylation in untreated HeLa cells and HeLa cells treated for 20 min with TSA. Using chromatin immunoprecipitation and DNA microarray (ChIP–chip) analysis we investigated a 1.2 Mb region on human chromosome 7, which includes the CFTR gene (Fig. 3; GEO accession number for ChIP–chip data: GSE29360).

We also analyzed the patterns of H3ac and H4ac in untreated Calu-3 cells (Fig. 3). CFTR is active in Calu-3 cells and localizes in the nuclear interior [Zink et al., 2004]. In contrast, CFTR is inactive in HeLa cells and localizes at the nuclear periphery. Thus, if hyperacetylation of histone H3 or H4 at particular sites of the CFTR locus would determine positioning in the nuclear interior, one would expect that these sites are more enriched in H3ac or H4ac in Calu-3 cells (compared to untreated HeLa cells). Furthermore, it would be expected that TSA treatment (which induces repositioning into the nuclear interior) would lead to corresponding enrichment of H3ac or H4ac at these sites also in HeLa cells.

Comparing the H3ac and H4ac data sets (Fig. 3) a higher number of significantly enriched sites was observed in case of the H3ac data (compared to H4ac) obtained with untreated and TSA-treated HeLa cells (significantly ($P < 0.001$) enriched sites are indicated in Fig. 3 in the two lines at the bottom of each lane; for further explanations see legend of Fig. 3). This can be possibly explained by a better signal-to-noise ratio of the H3ac data sets. However, it should be noted that the maximal level of H3ac is already reached after 20 min of TSA treatment, whereas the increase of H4ac is more slowly (Fig. 1). Overall, the results on the patterns of H3ac and H4ac in untreated HeLa cells obtained here were similar to the data obtained by the ENCODE project (http://genome.ucsc.edu/ENCODE/) and only some minor differences were observed (Supplementary Data, Fig. S3a). In general, the patterns of H3ac and H4ac enrichment were in untreated HeLa and Calu-3 cells in accordance with the patterns of gene activity. For instance, CAPZA2 (capping protein (actin filament) muscle Z-line, alpha 2; NM_006136.2, gene ID 830) and ST7 (suppressor of tumorigenicity protein 7; NM_021908.2, gene ID 7982) were active in both cell types [see Zenklusen et al., 2001 and http://bioinfo2.weizmann.ac.il/cgi-bin/genenote/home_page.pl] and the promoters of these genes were highly enriched in H3ac and H4ac. CFTR was not expressed at detectable levels in the HeLa cells used by us (no signal obtained by qPCR after 35 cycles, $n = 3$), but was expressed in Calu-3 cells. Accordingly, the CFTR promoter was highly enriched in H3ac and H4ac only in Calu-3 cells. Especially enrichment of H3ac was prominent (broad cluster with up to 18-fold enrichment) and the observation that H3ac is present at higher levels than H4ac at this site in Calu-3 cells is in accordance with previous data [Blackledge et al., 2007]. Although some significant enrichment of H3ac could be also detected at the CFTR promoter in untreated HeLa cells the levels of enrichment remained low (~2-fold). In addition, the 3′ end of CTTNBP2 was significantly enriched in H3ac and H4ac in both cell types (untreated), although the levels of enrichment were significantly higher in Calu-3 cells. Further, the 3′ end of MET (mesenchymal epithelial transition factor; NM_000245.2, gene ID 4233) and adjacent intergenic regions showed broad clusters of H3ac and H4ac enrichment in both cell types.

At the CFTR locus we observed sites that were more highly enriched in H3ac and/or H4ac in Calu-3 cells (compared to untreated HeLa cells) mainly at the promoter region (Fig. 3, lanes 2 and 4, red). A few additional sites could be found in the middle and second half of CFTR. In addition, prominent clusters of sites enriched in H3ac and H4ac were observed in Calu-3 cells upstream of the ASZ1 (ankyrin repeat, SAM and basic leucine zipper domain-containing protein 1; NM_130768.1, gene ID 136991) promoter in the intergenic region between ASZ1 and CFTR (Fig. 3, lanes 2 and 4). These two sites were overlapping with DNase I hypersensitive sites (DHS) that have previously been identified in CFTR-expressing primary cells [Ott et al., 2009].

For a better overview, all sites that were significantly enriched in H3ac or H4c under the different conditions and the overlaps between these sites are also displayed in Figure 4. About 90% of the sites that showed significant enrichment in H4ac in untreated HeLa cells were also significantly enriched in H3ac (Fig. 4a, lanes 1–3).

TSA-INDUCED CHANGES OF HISTONE ACETYLATION PATTERNS

Next, we addressed how treatment with TSA changed the patterns of histone H3 and H4 acetylation in HeLa cells. The ChIP–chip data obtained after 20 min of TSA treatment are displayed in Figure 3 (pink). For a better overview sites showing significant enrichment in

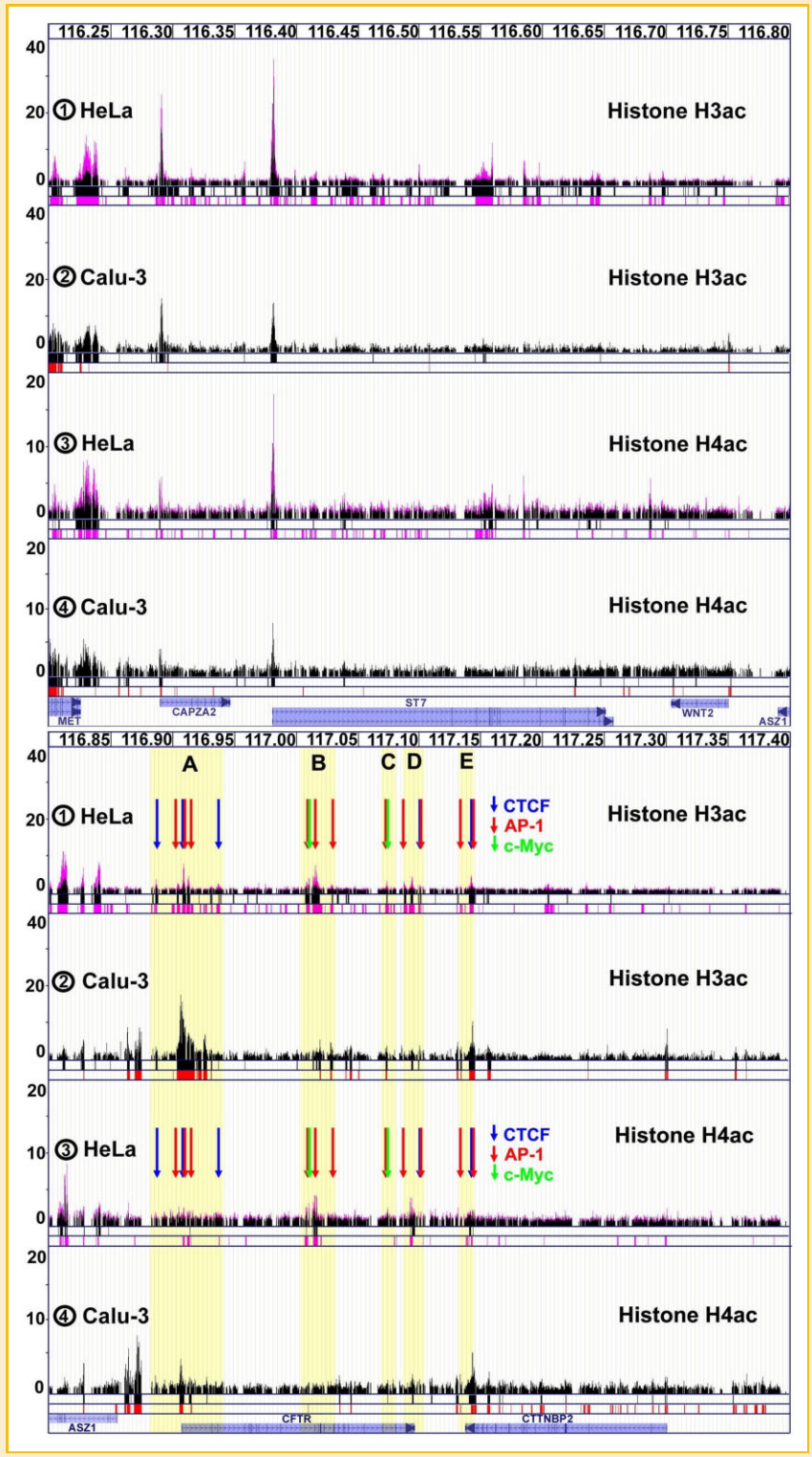

Fig. 3. Patterns of H3ac and H4ac determined by ChIP–chip. The genomic positions on chromosome 7 (116.2–117.4 Mb, hg18 assembly) are indicated at the top of each part of the figure. The genes (RefSeq, http://www.ncbi.nlm.nih.gov/RefSeq/) are shown at the bottom (blue). Exons are denoted by vertical bars and the direction of transcription is indicated by arrowheads at the 3′ ends of the genes. The profiles in lanes 1–4 show the mean values of the fluorescence intensities of the probe signals obtained with antibodies against H3ac or H4ac. The data were normalized to the values obtained with an antibody against histone H3 (scale on *y*-axis). Lane 1 (HeLa cells) and lane 2 (Calu-3 cells) show the profiles obtained for H3ac. Lane 3 (HeLa cells) and lane 4 (Calu-3 cells) show the profiles obtained for H4ac. Profiles obtained with untreated cells are shown in black and profiles derived from TSA-treated cells are displayed in pink (overlaid; only HeLa cells were treated with TSA). Bars in the two lines at the bottom of each lane denote significantly ($P < 0.001$) enriched sites. Black bars indicate sites that are significantly enriched in H3ac or H4ac in untreated cells (compared to the overall corresponding data set). Pink bars denote sites that are significantly enriched after TSA treatment (compared to corresponding data from untreated cells). Red bars highlight regions that are significantly more enriched in Calu-3 cells (compared to untreated HeLa cells). Regions A–E are highlighted in yellow. The arrows in these regions point to all CTCF (blue), AP-1 (red) and c-Myc (green) binding sites mapped by the ENCODE project in HeLa cells in CFTR and adjacent regions. [Color figure can be seen in the online version of this article, available at http://wileyonlinelibrary.com/journal/jcb]

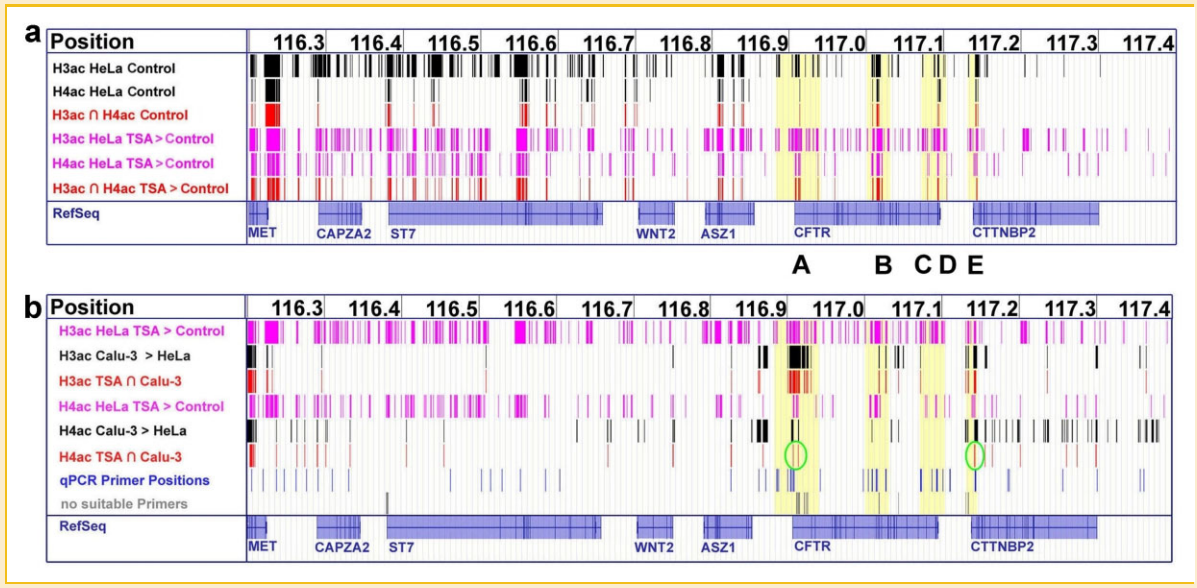

Fig. 4. Sites that are significantly enriched in H3ac or H4ac and their overlap. The genomic positions (Mb) are indicated at the top of panels a and b. The genes (RefSeq) are shown at the bottom (blue, vertical lines denote exons). Regions A–E are highlighted in yellow. a: The first two lanes (black) show sites significantly enriched in H3ac (lane 1) or H4ac (lane 2) in untreated HeLa cells (identical with the black lines at the bottom of lanes 1 and 3 in Fig. 3). Lane 3 (red) shows overlapping positions that are enriched in H3ac as well as in H4ac in untreated HeLa cells. Lanes 4 and 5 (pink) show sites that become significantly more enriched in H3ac (lane 4) or H4ac (lane 5) in HeLa cells after TSA treatment as compared to untreated control cells (identical with the pink lines at the bottom of lanes 1 and 3 in Fig. 3). Lane 6 (red) shows overlapping positions that become significantly more enriched in H3ac as well as in H4ac in HeLa cells after TSA treatment. b: Lane 1 (pink) shows sites that are significantly more enriched in H3ac in HeLa cells after TSA treatment (identical with lane 4 of panel a). Lane 2 (black) displays regions that are more highly enriched in H3ac in Calu-3 cells as compared to untreated HeLa cells (red in lane 2 of Fig. 3). Lane 3 (red) denotes overlapping positions that are more highly enriched in H3ac in TSA-treated HeLa cells and in Calu-3 cells as compared to untreated HeLa cells. Lane 4 (pink) shows sites that are significantly more enriched in H4ac in HeLa cells after TSA treatment (identical with lane 5 of panel a). Lane 5 (black) displays regions that are more highly enriched in H4ac in Calu-3 cells as compared to untreated HeLa cells (red in lane 4 of Fig. 3). Lane 6 (red) denotes overlapping regions that are more highly enriched in H4ac in TSA-treated HeLa cells and in Calu-3 cells as compared to untreated HeLa cells. Sites that are more highly enriched (compared to untreated HeLa cells) in H3ac as well as in H4ac under all conditions where CFTR localizes in the nuclear interior (TSA-treated HeLa cells and Calu-3 cells) are marked with green circles. Lane 7 (blue) denotes 63 primer positions used for validation of the ChIP–chip data (identical with the primer positions shown in Fig. 5). Lane 8 (gray) shows positions for which no suitable qPCR primers could be identified. [Color figure can be seen in the online version of this article, available at http://wileyonlinelibrary.com/journal/jcb]

H3ac or H4ac after TSA treatment are also displayed in Figure 4a (lanes 4 and 5, pink; overlap displayed in lane 6 (red)).

The data revealed that TSA treatment did not lead to uniform histone hyperacetylation. A significant TSA-induced increase in the levels of histone H3 and H4 acetylation (Fig. 3, pink bars) occurred often at sites that were already significantly enriched in H3ac or H4ac before TSA treatment (Fig. 3, black bars), as well as at additional sites. Especially regions that showed already high levels of H3ac or H4ac enrichment before TSA treatment were particularly highly enriched after TSA treatment. Such regions included the 3′ end of MET and adjacent intergenic regions, the promoters of CAPZA2 and ST7 and some sites within ASZ1.

Within CFTR and adjacent regions sites that showed significant TSA-induced increases in the levels of H3ac and H4ac clustered in five regions, which are designated A–E in Figures 3 and 4 and are highlighted in yellow. Region A corresponds to the promoter and surrounding regions (~50 kilo base pairs (kb)). B is in the middle of the CFTR and C and D are located at its 3′ end. E maps to the 3′ end of CTTNBP2. With one exception all of the sites that were significantly more enriched in H3ac as well as H4ac after TSA treatment mapped to regions A–E (Fig. 4a, lane 6, red). Additional sites that showed significant increases only in H3ac after TSA treatment could be also observed outside of regions A–E. However, sites that were more strongly enriched in H3ac (twofold and above) and were detectable as distinct peaks in the profile were located in regions A–E (Fig. 3, lane 1, pink; the H3ac profile of the CFTR gene and adjacent regions is also shown enlarged in Fig. 5a). Almost all of these distinct peaks of increased H3ac enrichment (after TSA treatment) corresponded to binding sites for regulatory factors (AP-1, c-Myc, and CTCF binding sites mapped in HeLa cells by the ENCODE project are marked in Fig. 3 by arrows (lanes 1 and 3)).

A corresponding clear correlation between binding sites for regulatory factors and TSA-induced histone hyperacetylation was not observed in case of H4ac (Fig. 3, lane 3). As it is known that HNF1α plays a role in CFTR regulation [Mouchel et al., 2004] and TSA-induced histone hyperacetylation [Paul et al., 2007] at the CFTR locus one might wonder how the patterns of histone hyperacetylation observed here were related to HNF1α binding sites. However, HNF1α expression could not be detected by qPCR in the HeLa cells used here (40 cycles, $n = 3$).

Generally, we observed a clear correlation between transcription factor (TF) binding sites (mapped by the ENCODE project) and TSA-induced patterns of H3ac enrichment in HeLa cells (Supplementary Data, Fig. S3). With one exception, the major clusters of TF binding sites mapped within the CFTR gene and adjacent areas to regions A–E (Supplementary Data, Fig. S3).

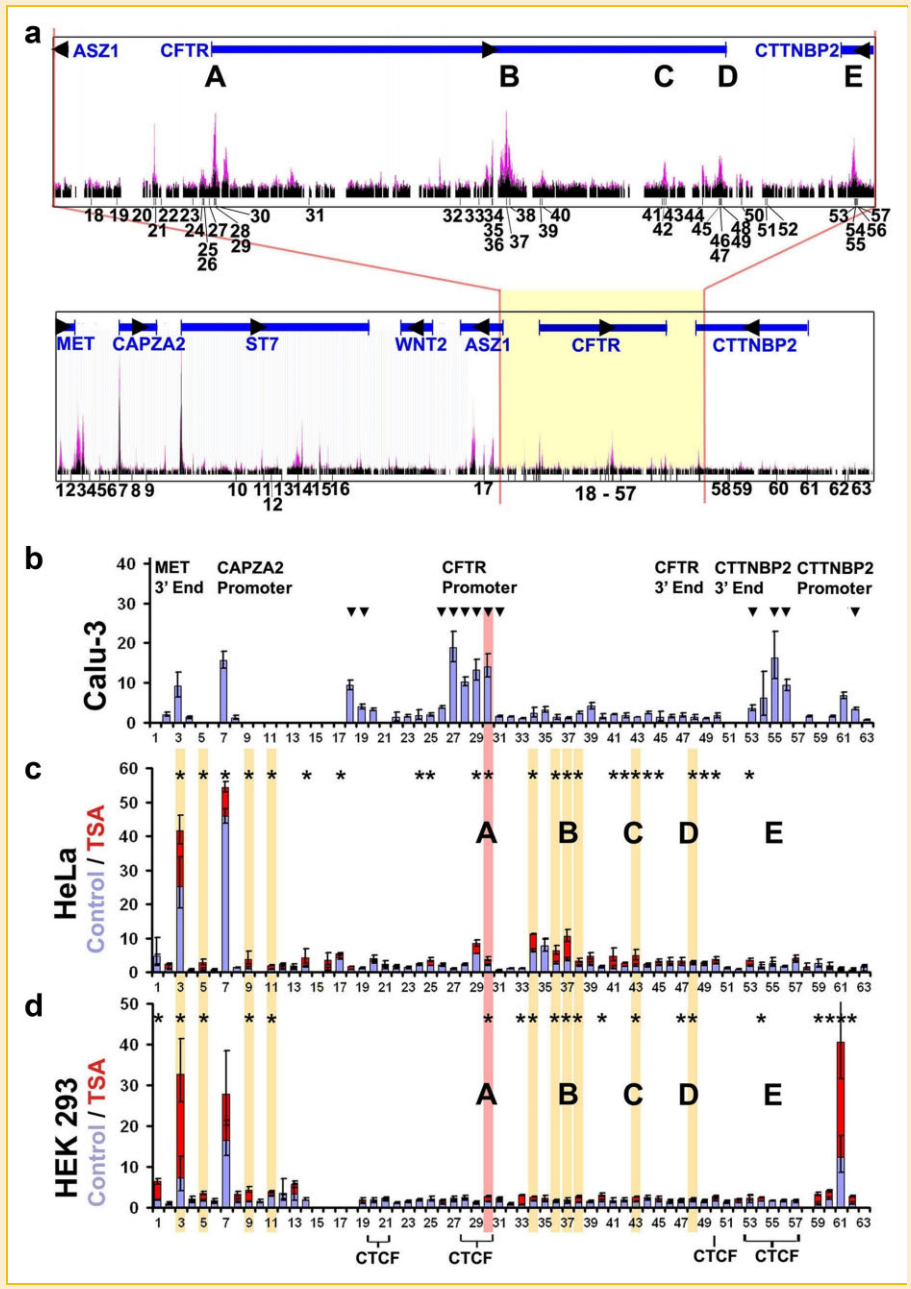

Fig. 5. Validation of the H3ac ChIP–chip data by ChIP–qPCR and identification of sites that are consistently enriched in H3ac when CFTR localizes in the nuclear interior. Sixty-three qPCR primer pairs (numbered 1–63) were used. Regions A–E are indicated. a: The positions of the primers relative to the genes (blue, black arrowheads indicate the direction of transcription) are shown. Panel a shows in addition the HeLa H3ac profiles (untreated: black; TSA-treated: pink) obtained by ChIP–chip (similar as in lane 1 of Fig. 3). The CFTR gene and adjacent areas are highlighted in yellow and are shown enlarged at the top. Panels b–d show the enrichment of H3ac (relative to histone H3; scale on *y*-axis) at the primer positions indicated on the *x*-axis. Positions 3 (adjacent to 3′ end of MET) and 7 (CAPZA2 promoter) were used as positive controls, whereas other positions (e.g., 6 and 31) were used as negative controls. The bars show the mean ± SEM (n = 3). The bars displaying data from untreated control cells (blue) are overlaid with the bars showing data from TSA-treated cells (red). Calu-3 (b), HeLa (c), and HEK 293 (d) cells were analyzed. Sites that are significantly ($P < 0.05$) more enriched in H3ac in Calu-3 cells as compared to untreated HeLa and HEK 293 cells are marked with black arrowheads. Sites in HeLa or HEK 293 cells that display a significant increase in H3ac enrichment after TSA-treatment are marked with black asterisks. Overlapping sites that are significantly more enriched in H3ac (compared to corresponding untreated cells) in both TSA-treated HeLa and HEK 293 cells are labeled with yellow bars. Sites that are significantly more enriched in H3ac (compared to untreated HeLa and HEK 293 cells) under all conditions where CFTR localizes in the nuclear interior (Calu-3 cells and TSA-treated HeLa and HEK 293 cells) are marked with a light-red bar. This condition applies only to site 30, which maps to a CTCF site in the first intron of CFTR (close to the CFTR promoter; CTCF sites are indicated at the bottom). [Color figure can be seen in the online version of this article, available at http://wileyonlinelibrary.com/journal/jcb]

As DHS usually represent sites that are occupied by TFs and other regulatory factors it is not surprising that there is a good match between TF binding sites and DHS mapped by the ENCODE project or by Ann Harris and co-workers [Mouchel et al., 2004; McCarthy and Harris, 2005; Blackledge et al., 2007; Blackledge et al., 2009; Ott et al., 2009] (Supplementary Data, Fig. S3a). From 17 DHS that were mapped by Ann Harris and co-workers in the CFTR region 11 overlapped with sites showing significant TSA-induced increases in H3ac in HeLa cells (Table I; note that these 17 DHS do not represent a complete list of all DHS that have been mapped at the CFTR locus). Only 5 of these 17 DHS corresponded to sites that showed significant enrichment of H3ac in untreated HeLa cells (Table I). In untreated Calu-3 cells, where CFTR is active, 13 regions enriched in H3ac overlapped with previously identified DHS. Together, the results shown in Table I suggest that regulatory elements show increased histone acetylation, in agreement with previous studies [Roh et al., 2007]. The patterns of histone acetylation can be useful for identifying regulatory elements and our findings suggest that TSA treatment enhances the sensitivity of detection if the gene of interest is not expressed. It is worth mentioning that DHS are often cell type-specific and the 17 DHS included here were mapped by using various cell types from different tissues.

IDENTIFICATION OF SITES THAT ARE CONSISTENTLY HYPERACETYLATED WHEN CFTR LOCALIZES IN THE NUCLEAR INTERIOR

If histone hyperacetylation at specific sites would be involved in the regulation of nuclear positioning it would be expected that such sites display consistent enrichment in H3ac and/or H4ac in situations where CFTR localizes in the nuclear interior. In order to identify such sites, we compared the patterns of TSA-induced histone hyperacetylation in HeLa cells with sites enriched in H3ac or H4ac in Calu-3 cells. Figure 4b displays all regions that show significant increases in H3ac or H4ac in HeLa cells after TSA treatment (lanes 1 and 4, pink). Lanes 2 and 5 (black) display those sites that are more highly enriched in H3ac or H4ac in Calu-3 cells compared to untreated HeLa cells. Lanes 3 and 6 display the overlapping sites (red) with regard to H3ac or H4ac.

In case of H3ac many overlapping sites (Fig. 4b, lane 3, red) were found around the promoter (region A) and some additional sites were observed in regions B, C and E (one site was located between B and C). In case of H4ac only three overlapping sites were identified (Fig. 4b, lane 6, red). Two of them were located adjacent to the promoter region and one additional site was located in region E. These three sites were also significantly enriched in H3ac in Calu-3 cells and TSA-treated HeLa cells (compared to untreated HeLa cells). Thus, the ChIP–chip data indicated that these sites, which are highlighted by green circles in Figure 4b, were enriched in H3ac and H4ac under all conditions where CFTR localized in the nuclear interior.

The first of these sites in region A is a CTCF binding site (mapped by the ENCODE project and in this study; see Fig. S7). This site is located in the first kilobase pair (kb) of intron 1 and also maps close to the promoter (distance to promoter < 1.5 kb, the first exon of CFTR is very short). Also the site in region E corresponds to a CTCF binding site. This site is located in the last intron of CTTNBP2 and has been identified as ubiquitous DHS unrelated to CFTR expression by Ott et al. [2009]. We were not able to assign any specific function to the second consistently hyperacetylated site in region A.

The next series of experiments was performed in order to validate these results obtained by ChIP–chip by using ChIP–qPCR. Sixty-three sites were tested by using specific primer pairs and the positions of these sites are shown in Figure 5a. ChIP was performed with untreated Calu-3 cells, untreated (control) and TSA-treated (20 min) HeLa cells and untreated and TSA-treated human embryonic kidney (HEK) 293 cells. Including HEK 293 cells allowed us to further identify elements that became consistently hyperacetylated when CFTR localized in the nuclear interior. We could show before that CFTR is not expressed in HEK 293 cells and is driven from the nuclear periphery into the nuclear interior by TSA treatment [Zink et al., 2004; Englmann et al., 2005]. Thus, CFTR showed in this cell line the same behavior as in HeLa cells and under the conditions used CFTR localized in the nuclear interior

TABLE I. Overlap of DHS With Sites Significantly Enriched in H3ac

	DHS	HeLa H3ac, TSA	HeLa H3ac, untreated	Calu-3 H3ac, untreated
1	−44 kb 5′			
2	−35 kb 5′			
3	−20.9 kb 5′			
4	Promoter			
5	185 + 10 kb intron 1			
6	1716 + 13.2/13.7 kb intron 10			
7	1716 + 23 kb intron 10			
8	1811 + 0.8 kb intron 11			
9	3600 + 1.6 kb intron 18			
10	3600 + 10 kb intron 18			
11	3849 + 12.5 kb intron 19			
12	4374 + 1.3 kb intron 23			
13	+6.8 kb 3′			
14	+15.6 kb 3′			
15	+21.5 kb 3′			
16	+36.6 kb 3′			
17	+48.9 kb 3′			

The table lists 17 DHS previously mapped by the Ann Harris and co-workers [Mouchel et al., 2004; McCarthy and Harris, 2005; Blackledge et al., 2007, 2009; Ott et al., 2009]. Overlap with sites significantly enriched in H3ac in untreated HeLa or Calu-3 cells is indicated by gray cells, as well as overlap with sites where a significant increase in H3ac is observed after TSA treatment of HeLa cells.

in TSA-treated HeLa and HEK 293 cells as well as in untreated Calu-3 cells.

Figure 5b–d shows that the ChIP–qPCR results obtained for H3ac were consistent with the ChIP–chip data. For instance, in untreated cells (blue bars) high levels of H3ac enrichment were observed close to the 3′ of MET (probe 3) and at the CAPZA2 promoter (probe 7), which further increased after TSA-treatment (red bars). Sites that were significantly higher enriched in H3ac in Calu-3 cells than in untreated HeLa and HEK 293 cells are marked with black arrowheads in Figure 5b. Such sites mapped to the CFTR promoter and adjacent regions, as well as to the promoter and the 3′ end of CTTNBP2, which is consistent with the ChIP–chip data. The promoter of CTTNBP2 was also enriched in H3ac in untreated HEK 293 cells but not in HeLa cells. These data are consistent with the fact that CTTNBP2 is expressed in Calu-3 and HEK 293 cells [Zink et al., 2004] but not in HeLa cells (3×10^{-4} % of glyceraldehyde-3-phosphate dehydrogenase expression as determined by qPCR). Positions 18 and 19 mapped to two previously identified DHS present in CFTR-expressing primary cells [Ott et al., 2009]. The ChIP–chip data revealed at these positions in Calu-3 cells significant enrichment of H3ac and H4ac (Fig. 3) and thus also in this case the ChIP–chip and ChIP–qPCR data are in agreement.

Also consistent with the ChIP–chip data, a significant increase in the enrichment in H3ac was observed in HeLa cells after TSA treatment (sites that showed significant increase in H3ac after TSA treatment, as compared to untreated cells, are marked by asterisks in Fig. 5c,d) at sites clustering in regions A–E, as well as at additional sites. Other sites that were used as negative controls (e.g., 31–33) remained unaffected.

Sites that showed significant increase in H3ac after TSA treatment in HeLa as well as in HEK 293 cells are marked by yellow bars in Figure 5. Sites that fulfilled this condition and overlapped in addition with sites that showed significantly higher levels of H3ac in Calu-3 cells (compared to untreated HeLa and HEK 293 cells) are labeled by light-red bars in Figure 5b–d. This condition applied only to one site, which was the CTCF site in intron 1 close to the CFTR promoter. This site had also been identified as being a consistently hyperacetylated site by the ChIP–chip analysis and corresponds to the first of the three sites encircled in green in Figure 4b. Sequence analysis (data not shown) revealed that this site contained a conserved CCCTC motif flanked by GA-rich motifs.

The CTCF sites covered by the primer pairs used here are highlighted in Figure 5. Two of these sites [Blackledge et al., 2007, 2009] do not show increased levels of H3ac at all (position 20/21) or display a cell-type specific increase after TSA-treatment (position 50) (Fig. 5b–d). Another CTCF site is located at the 3′ end of CTTNBP2 (region E, probes 53–57). This site has been identified as being consistently hyperacetylated by the ChIP–chip analysis (encircled in Fig. 4b). The ChIP–qPCR analysis revealed consistently increased levels of H3ac in Calu-3 and TSA-treated HeLa cells at position 53. In HEK 293 cells TSA treatment induced significantly increased levels of H3ac at position 54, which is 162 bp away from position 53. As this site is located within CTTNBP2 and maps to a ubiquitous DHS that is unrelated to CFTR expression [Ott et al., 2009] it is unlikely that the increased levels of H3ac observed here are related to the positional regulation of CFTR. It is worth mentioning that the nuclear positioning of CTTNBP2 and CFTR is independent [Zink et al., 2004 and see Fig. 7].

The third site, that had been identified by the ChIP–chip analysis as consistently hyperacetylated in situations where CFTR localized in the nuclear interior (second site in region A, encircled in Fig. 4b) could not be confirmed by ChIP–qPCR as it was not possible to identify specific primer pairs (Fig. 4b, gray).

A similar ChIP–qPCR analysis, as performed with regard to H3ac, was also performed for H4ac (Fig. S4). Overall, the data were in agreement with the results obtained so far. However, a specific site that displayed consistently increased levels of H4ac in all three cell lines under conditions where CFTR localized in the nuclear interior could not be identified. This applied also to the CTCF site in the first CFTR intron and thus consistent histone H4 hyperacetylation at this site could not be confirmed.

As an earlier study [Luco et al., 2008] suggested that histone methylation could play a role in gene positioning we also addressed whether TSA treatment led to changes in the patterns of histone methylation in HeLa cells. ChIP–chip analyses were performed with the same DNA microarrays as described above and antibodies against histone H3 tri-methylated at lysine 4 (H3K4me3), H3K9me3, and H3K27me3. Cells were left untreated or were treated for 20, 40, and 60 min with TSA. The results (Supplementary Data, Fig. S5) revealed no substantial TSA-induced changes in the patterns of H3K4me3, H3K9me3, and H3K27me3. However, slight changes could be observed at some sites and for these and other sites (e.g., in the promoter region) specific primer pairs were generated in order to validate the data by ChIP–qPCR. Figure S6 (Supplementary Data) summarizes the ChIP–qPCR results. For all three histone H3 modifications and the 30 sites tested we observed at only one site a significant change ($P < 0.05$) with regard to the levels of H3K9me3 after 20 min of TSA treatment. No specific function could be assigned to this site. Overall, the data showed that the patterns of H3K4me3, H3K9me3, and H3K27me3 remained largely unaffected by TSA treatment. In addition, the data showed relatively high levels of H3K9me3 at the CFTR locus, which is consistent with the fact that the gene was not expressed in the HeLa cells used here.

CTCF AND A-TYPE LAMINS ARE ESSENTIAL FOR THE PERINUCLEAR POSITIONING OF CFTR

Given the consistently increased levels of H3ac at the CTCF site located close to the CFTR promoter in situations where CFTR localized in the nuclear interior we asked whether CTCF could be involved in the positional regulation of CFTR. To address this question we knocked down CTCF in HeLa and HEK 293 cells by using CTCF-specific small interfering (si)RNAs (Fig. 6). In both cell types this treatment led to ~75% reduction in the amounts of CTCF as determined by immunoblotting and densitometric analysis.

Next, we tested by FISH and 2D erosion analysis whether CTCF knockdown affected the radial positioning of CFTR. Figure 7a shows that CFTR occupied in HeLa cells and HEK 293 cells significantly ($P < 0.05$) more interior positions after CTCF knockdown. Control experiments with unspecific siRNA revealed that these effects were only induced by the CTCF-specific siRNA but not by unspecific siRNA (Supplementary Data, Fig. S1b).

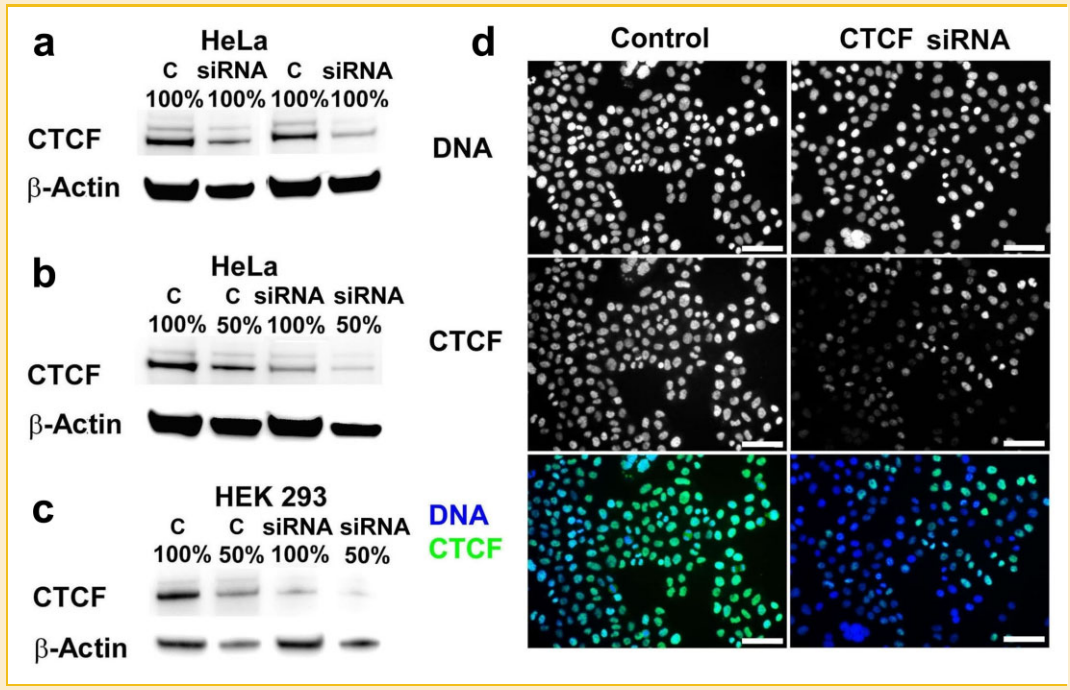

Fig. 6. Panels a–c show immunoblots with lysates from HeLa and HEK 293 cells. The cells were either untreated (control: c) or treated with CTCF-specific siRNA (siRNA). One hundred percent and 50% refer to the relative amounts of cell lysate loaded. For detection antibodies against CTCF and β-actin (loading control) were used. Results from two independent CTCF knock down experiments performed with HeLa cells are shown in panels a and b. The images in (d) show HeLa cells after immunofluorescent staining with an anti-CTCF antibody. Untreated control cells (left-hand panels) or cells treated with CTCF-specific siRNA (right-hand panels) were used. DAPI staining is shown at the top and in blue in the merges at the bottom. The CTCF-specific immunofluorescence is shown in the middle and in green at the bottom. Scale bar: 50 μm. [Color figure can be seen in the online version of this article, available at http://wileyonlinelibrary.com/journal/jcb]

In addition, we compared the effects of CTCF knockdown to the TSA-induced effects on gene positioning. Figure 7a shows that the effects of CTCF knockdown and TSA-treatment were similar in both cell types and after both treatments CFTR localized at significantly ($P < 0.05$) more interior positions. Any significant differences between the effects of CTCF knockdown and TSA treatment on the positioning of CFTR could not be detected.

In agreement with our previous results [Zink et al., 2004] the effects on gene positioning were specific for CFTR and the neighboring genes ASZ1 and CTTNBP2 were not affected (Fig. 7a). Control experiments with the β-globin locus revealed that TSA-treatment or CTCF knockdown had also no significant effects on the positioning of this locus (Supplementary Data, Fig. S1c). The observations that CTCF knockdown affects positioning in a locus-specific manner and does not lead to global disturbance of gene positioning are in agreement with previous findings [Ottaviani et al., 2009b].

Release of CTCF binding by TSA treatment could explain the similar effects of TSA treatment and CTCF knockdown. We determined the effects of TSA treatment on CTCF binding in HeLa and HEK 293 cells by ChIP–qPCR (Fig. S7). The results revealed that either 20 min or 10 h of TSA treatment did not lead to a significant decrease of CTCF binding ($P > 0.05$). This applied also to positions 29 and 30, which are about 300 bp apart from each other. Position 29 appeared to harbor the major CTCF binding site (Fig. S7) in the first CFTR intron adjacent to the promoter. Significantly increased levels of H3ac in Calu-3 cells (compared to untreated HeLa cells) and in TSA-treated cells were observed at positions 29 (Calu-3 cells and TSA-treated HeLa cells, Fig. 5) and 30 (Calu-3 cells and TSA-treated HeLa and HEK 293 cells, Fig. 5). Altogether, these results show that the observed effects of TSA on gene positioning could not be explained by release of CTCF from critical binding sites.

As our data revealed that TSA treatment of HeLa cells induced relatively high levels of histone acetylation at several sites within ASZ1 (Fig. 3, lanes 1 and 3) and at a CTCF site in the last intron of CTTNBP2, the results showed that just increased histone acetylation at CTCF sites or at other sites is not sufficient to induce gene relocalization. As the neighboring genes contained CTCF sites (Fig. S7) the result that CTCF knockdown did not affect the positioning of neighboring genes suggested that CTCF does not determine gene positioning directly, but that rather site-specific CTCF-associated factors play an important role. An obvious candidate would be a CTCF-associated HDAC, as inhibition of HDACs or CTCF knockdown have the same effect on CFTR positioning. The data showed that the CTCF site adjacent to the CFTR promoter is associated with an HDAC, otherwise TSA treatment would not lead to increased levels of H3ac at this site. It should be noted that increase in H3ac was not consistently observed at different CTCF sites after TSA treatment (Fig. 5), which suggested that association with an HDAC only occurred at specific CTCF sites, including the one adjacent to the CFTR promoter.

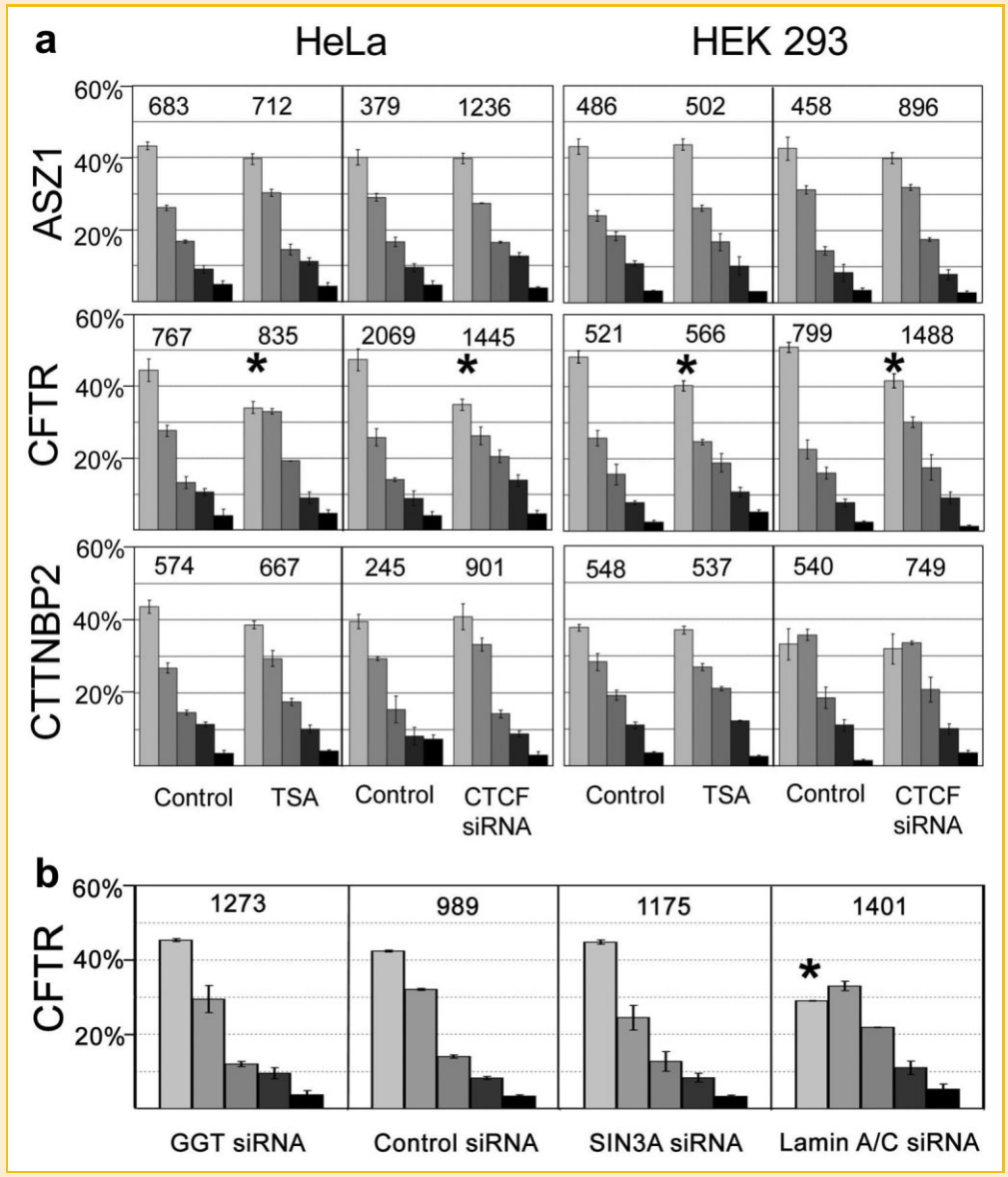

Fig. 7. Effects of TSA treatment and RNAi knockdown on gene positioning. a: HeLa and HEK 293 cells were treated with TSA or CTCF-specific siRNA or were left untreated (control). The positioning of CFTR and of the neighboring genes ASZ1 and CTTNBP2 was determined by FISH and 2D erosion analysis. For further explanations of diagrams see legend of Figure 2. Asterisks denote significant ($P < 0.05$) changes in the numbers of FISH signals. b: HeLa cells were treated with siRNA specific for γ-glutamyltransferase (GGT, control), unspecific control siRNA or siRNA specific for SIN3A. In addition, HeLa cells were treated with lamin A/C-specific siRNA. The positioning of CFTR was determined by FISH and erosion analysis. Asterisks denote significant ($P < 0.05$) changes in the numbers of FISH signals.

Using HeLa cell extracts it has been shown that CTCF binds the co-repressor SIN3A, which correlates with the ability to recruit HDAC activity [Lutz et al., 2000]. These data suggested that CTCF recruits a SIN3A–HDAC complex. Here, we found that knockdown of SIN3A does not influence the positioning of CFTR (Fig. 7b), which showed that a potential SIN3A–HDAC complex recruited by CTCF is not involved in the positioning of CFTR.

Previous studies have shown that perinuclear positioning of the human D4Z4 repeat depended on CTCF as well as on A-type lamins [Ottaviani et al., 2009ab]. Knockdown of lamin A/C (Fig. S8) revealed that also the perinuclear positioning of CFTR depended on A-type lamins (Figs. 7b and S9). Together, the results showed that perinuclear positioning of the inactive CFTR gene depended on a mechanism involving CTCF, A-type lamins and an active HDAC, which acted at the nuclear periphery on a CTCF binding site adjacent to the CFTR promoter.

DISCUSSION

Here, we addressed molecular mechanisms regulating radial gene positioning by using TSA-induced repositioning of CFTR as a model

system. We show that first significant changes in the positioning of CFTR occurred after 20 min of TSA treatment. At this time point also significant increases in the global levels of H3ac and H4ac could be observed, as well as significant increases in the levels of H3ac and H4ac at specific sites within a 1.2 Mb region on human chromosome 7 harboring the CFTR gene. Major changes in the patterns of H3K4me3, H3K9me3, and H3K27me3 within this region were not observed.

The levels of H3ac or H4ac did not increase uniformly after TSA treatment in the 1.2 Mb region. In particular, increases in H3ac occurred at the CFTR locus mainly at binding sites for regulatory factors. These findings are in agreement with the results of Paul et al. [2007], although it should be noted that in this study different cell lines and transcription factors were addressed than those investigated here. The binding sites for regulatory factors that showed increased levels of H3ac in our study included a CTCF binding site adjacent to the CFTR promoter (within the first intron of CFTR). This was the only site that showed consistently increased levels of H3ac in situations where CFTR localized in the nuclear interior (either in TSA-treated cells or in untreated cells where CFTR was active).

Furthermore, the data revealed that CTCF was essential for positioning of CFTR at the nuclear periphery, as well as lamin A/C. These results were consistent with earlier findings showing that CTCF as well as A-type lamins were essential for the perinuclear positioning of the D4Z4 repeat [Ottaviani et al., 2009b]. Lamin A/C and CTCF have been co-purified from HeLa cell extracts [Yusufzai et al., 2004] suggesting functional interactions between these proteins.

The fact that knockdown of CTCF had the same effect on CFTR positioning as TSA treatment revealed that both, CTCF and an active HDAC contributed to the mechanism that positioned CFTR at the nuclear periphery. Thus, this mechanism comprised at least three components: lamin A/C, CTCF and an active HDAC. The HDAC did not appear to be associated to CTCF via SIN3A, but it interacted with the CTCF binding site adjacent to the promoter. Otherwise, increased levels of H3ac would not have been observed at this site after TSA treatment. Furthermore, the HDAC appeared to be mainly active at the nuclear periphery because increased levels of H3ac were also observed at the CTCF site in non-TSA-treated Calu-3 cells, where CFTR localized in the nuclear interior. For HDAC3 it has been shown that it interacts at the nuclear periphery with LAP2β [Somech et al., 2005]. Thus, the HDAC activity observed here was probably recruited to the nuclear periphery by interacting with other proteins at the nuclear lamina. Together, the findings suggest that A-type lamins, an active HDAC and CTCF bound to a site adjacent to the CFTR promoter were components of a complex at the nuclear periphery that controlled the positioning of the inactive CFTR gene (Fig. 8).

HDAC inhibition led to release of CFTR from the nuclear periphery, which revealed that HDAC activity was required for maintaining the gene at this position. Whether the observed increase of H3ac played an essential role in release of CFTR from the nuclear periphery is currently unclear. Probably the HDAC acted on histone H3 in addition other substrates as, for instance, other members of the putative CTCF/A-type lamin/HDAC complex, which might also contain additional proteins. Our data showed that also CTCF was

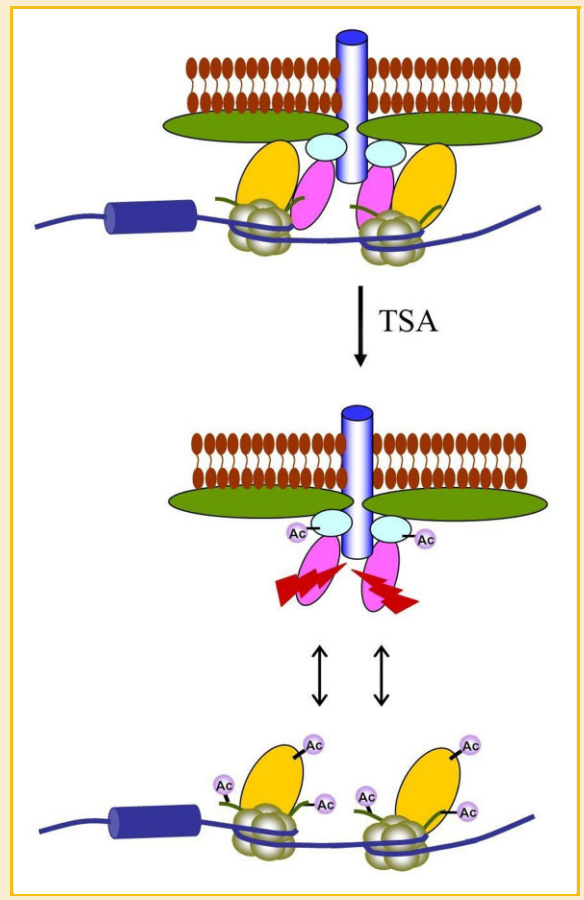

Fig. 8. Model. The lamina underlying the inner nuclear membrane (brown) is formed by lamins (lamin A/C: green) and lamina-associated proteins. A subset of lamina-associated proteins consists of integral membrane proteins (white cylinder). We propose that lamin A/C forms a complex with CTCF (yellow) and an active HDAC (pink). The putative complex contains probably also other lamina-associated proteins (light blue). CTCF binds to DNA (blue line) at a site adjacent to the CFTR promoter (dark-blue cylinder). The DNA is assembled into nucleosomes (gray), which contain histone H3 (histone H3 tails: green). Inhibition of the HDAC (red arrows) by TSA treatment increases acetylation (Ac) of histone H3 tails and probably also of CTCF and other components of the putative complex. This might lead to disruption of the complex and release of CFTR from the nuclear periphery. TSA treatment does not impact DNA binding of CTCF. [Color figure can be seen in the online version of this article, available at http://wileyonlinelibrary.com/journal/jcb]

acetylated (Fig. S10) and is therefore a putative target. We propose that increased acetylation due to inhibition of the HDAC interacting with the CTCF site at the CFTR promoter led to disruption of a complex that tethered CFTR to the nuclear periphery and to subsequent release of the gene (Fig. 8). It would be critical now to identify the HDAC involved in these processes and to purify the proposed complex containing this HDAC.

In agreement with our data it has been shown before that the interaction of inactive genes with the lamina of Drosophila cells was disrupted by TSA treatment, which led to relocalization of such genes into the nuclear interior [Pickersgill et al., 2006]. Thus, previous studies revealed that in addition to lamins an active HDAC [Pickersgill et al., 2006] or CTCF [Ottaviani et al., 2009b] were

essential for perinuclear positioning. Our results revealed for the first time that all of these components are together involved in a mechanism regulating gene positioning. Together, our results and those of the previous studies also suggested that the mechanism is conserved and does not only act on CFTR.

Previous studies showed that A-type lamins are essential for nuclear and chromatin organization and the positioning of chromosomes and chromosomal domains [Taimen et al., 2009; Ottaviani et al., 2009b; Mewborn et al., 2010]. However, the effects on chromosome location appear to be cell type-specific and, for instance, little or no changes in chromosome location were detected in lymphoblastoid cell lines derived from patients with lamin A mutations [Meaburn et al., 2005]. It should also be noted that the positioning of CFTR is regulated at the level of the individual gene and is independent from changes in the positioning of surrounding chromosomal domains [see Zink et al., 2004 and Fig. 7].

The finding that CTCF at the 5′ end of CFTR interacted with an HDAC activity was in agreement with the fact that CFTR was not expressed in HeLa and HEK 293 cells [this study and Zink et al., 2004; Englmann et al., 2005]. CTCF has been shown before to act as repressor for certain genes and its repressive functions depended on its ability to recruit a functional HDAC [Lutz et al., 2000]. Together, the findings were consistent with a dual role for the HDAC activity at the CFTR promoter: (i) regulating gene positioning and (ii) regulating repressive chromatin structures. It should be noted that H3 hyperacetylation at the CFTR promoter is a hallmark of the active gene in the nuclear interior (Fig. 3, Calu-3 cells). In the scenario outlined here, recruitment of CFTR to the nuclear periphery would contribute to gene silencing, which would be in agreement with the findings of Somech et al. [2005]. In this study it was demonstrated that the nuclear envelope protein LAP2β acts as transcriptional repressor, induces histone H4 deacetylation and interacts with HDAC3 at the nuclear periphery.

In addition to the other results our data show that profiling of H3ac levels after TSA treatment is useful for identifying regulatory regions. Due to the particular interest in the regulatory elements of the human CFTR gene these elements have been intensely investigated and mapped by different methods including DHS mapping [see Smith et al., 1996; Moulin et al., 1999; Nuthall et al., 1999ab; McCarthy and Harris, 2005; Blackledge et al., 2007, 2009; Ott et al., 2009], chromosome conformation capture analysis [Blackledge et al., 2009; Ott et al., 2009; Gheldof et al., 2010] and comparative analyses of multi-species sequences [Thomas et al., 2003]. The results are largely consistent and similar regulatory regions have been identified by using different methods. The findings suggest that the DHS identified in various studies represent most of the important regulatory regions of the CFTR locus. Our results show that many of these regions can also be easily identified by their increases in the levels in H3ac after TSA treatment. Thus, TSA treatment and subsequent profiling of histone acetylation patterns appears to provide an alternative method for identifying regulatory regions, and this method has a higher sensitivity than profiling of the histone acetylation patterns in untreated cells [Roh et al., 2007], at least as long as the gene of interest is inactive (Table I, CFTR is inactive in HeLa cells but active in Calu-3 cells). Therefore, profiling of H3ac after TSA treatment might be particularly useful for the identification of regulatory elements in larger genomic regions containing a mixture of active and inactive genes. The sensitivity appears to be at least as high as DHS mapping as DHS are often cell type-specific and typically only a subset of all potential DHS can be detected in any given cell type.

ACKNOWLEDGMENTS

We thank Prof. Ann Harris (Northwestern University, Chicago, IL, USA) for help with experimental procedures and valuable comments on the manuscript.

REFERENCES

Bell AC, West AG, Felsenfeld G. 1999. The protein CTCF is required for the enhancer blocking activity of vertebrate insulators. Cell 98(3):387–396.

Blackledge NP, Carter EJ, Evans JR, Lawson V, Rowntree RK, Harris A. 2007. CTCF mediates insulator function at the CFTR locus. Biochem J 408(2):267–275.

Blackledge NP, Ott CJ, Gillen AE, Harris A. 2009. An insulator element 3′ to the CFTR gene binds CTCF and reveals an active chromatin hub in primary cells. Nucleic Acids Res 37(4):1086–1094.

Buck MJ, Nobel AB, Lieb JD. 2005. ChIPOTle: A user-friendly tool for the analysis of ChIP-chip data. Genome Biol 6(11):R97.

Cremer M, von Hase J, Volm T, Brero A, Kreth G, Walter J, Fischer C, Solovei I, Cremer C, Cremer T. 2001. Non-random radial higher-order chromatin arrangements in nuclei of diploid human cells. Chromosome Res 9:541–567.

Croft JA, Bridger JM, Boyle S, Perry P, Teague P, Bickmore WA. 1999. Differences in the localization and morphology of chromosomes in the human nucleus. J Cell Biol 145(6):1119–1131.

Englmann A, Clarke LA, Christan S, Amaral MD, Schindelhauer D, Zink D. 2005. The replication timing of CFTR and adjacent genes. Chromosome Res 13(2):183–194.

Fedorova E, Zink D. 2008. Nuclear architecture and gene regulation. Biochim Biophys Acta 1783(11):2174–2184.

Fedorova E, Zink D. 2009. Nuclear genome organization: Common themes and individual patterns. Curr Opin Genet Dev 19(2):166–171.

Ferrai C, de Castro IJ, Lavitas L, Chotalia M, Pombo A. 2010. Gene positioning. Cold Spring Harb Perspect Biol 2(6):a000588.

Gheldof N, Smith EM, Tabuchi TM, Koch CM, Dunham I, Stamatoyannopoulos JA, Dekker J. 2010. Cell-type-specific long-range looping interactions identify distant regulatory elements of the CFTR gene. Nucleic Acids Res 38(13):4325–4336.

Hark AT, Schoenherr CJ, Katz DJ, Ingram RS, Levorse JM, Tilghman SM. 2000. CTCF mediates methylation-sensitive enhancer-blocking activity at the H19/Igf2 locus. Nature 405(6785):486–489.

Ling JQ, Li T, Hu JF, Vu TH, Chen HL, Qiu XW, Cherry AM, Hoffman AR. 2006. CTCF mediates interchromosomal colocalization between Igf2/H19 and Wsb1/Nf1. Science 312(5771):269–272.

Luco RF, Maestro MA, Sadoni N, Zink D, Ferrer J. 2008. Targeted deficiency of the transcriptional activator hnf1alpha alters subnuclear positioning of its genomic targets. PLoS Genet 4(5):e1000079.

Lutz M, Burke LJ, Barreto G, Goeman F, Greb H, Arnold R, Schultheiss H, Brehm A, Kouzarides T, Lobanenkov V, Renkawitz R. 2000. Transcriptional repression by the insulator protein CTCF involves histone deacetylases. Nucleic Acids Res 28(8):1707–1713.

McCarthy VA, Harris A. 2005. The CFTR gene and regulation of its expression. Pediatr Pulmonol 40(1):1–8.

Meaburn KJ, Levy N, Toniolo D, Bridger JM. 2005. Chromosome positioning is largely unaffected in lymphoblastoid cell lines containing emerin or A-type lamin mutations. Biochem Soc Trans 33(Pt 6):1438–1440.

Mewborn SK, Puckelwartz MJ, Abuisneineh F, Fahrenbach JP, Zhang Y, MacLeod H, Dellefave L, Pytel P, Selig S, Labno CM, Reddy K, Singh H, McNally E. 2010. Altered chromosomal positioning, compaction, and gene expression with a lamin A/C gene mutation. PLoS ONE 5(12):e14342.

Mouchel N, Henstra SA, McCarthy VA, Williams SH, Phylactides M, Harris A. 2004. HNF1alpha is involved in tissue-specific regulation of CFTR gene expression. Biochem J 378(Pt 3):909–918.

Moulin DS, Manson AL, Nuthall HN, Smith DJ, Huxley C, Harris A. 1999. In vivo analysis of DNase I hypersensitive sites in the human CFTR gene. Mol Med 5(4):211–223.

Nuthall HN, Moulin DS, Huxley C, Harris A. 1999a. Analysis of DNase-I-hypersensitive sites at the 3′ end of the cystic fibrosis transmembrane conductance regulator gene (CFTR). Biochem J 341(Pt 3):601–611.

Nuthall HN, Vassaux G, Huxley C, Harris A. 1999b. Analysis of a DNase I hypersensitive site located −20.9kb upstream of the CFTR gene. Eur J Biochem 266(2):431–443.

Ohlsson R, Lobanenkov V, Klenova E. 2010. Does CTCF mediate between nuclear organization and gene expression? BioEssays 32(1):37–50.

Ott CJ, Blackledge NP, Kerschner JL, Leir SH, Crawford GE, Cotton CU, Harris A. 2009. Intronic enhancers coordinate epithelial-specific looping of the active CFTR locus. Proc Natl Acad Sci USA 106(47):19934–19939.

Ottaviani A, Rival-Gervier S, Boussouar A, Foerster AM, Rondier D, Sacconi S, Desnuelle C, Gilson E, Magdinier F. 2009a. The D4Z4 macrosatellite repeat acts as a CTCF and A-type lamins-dependent insulator in facio-scapulo-humeral dystrophy. PLoS Genet 5(2):e1000394.

Ottaviani A, Schluth-Bolard C, Rival-Gervier S, Boussouar A, Rondier D, Foerster AM, Morere J, Bauwens S, Gazzo S, Callet-Bauchu E, Gilson E, Magdinier F. 2009b. Identification of a perinuclear positioning element in human subtelomeres that requires A-type lamins and CTCF. EMBO J 28(16): 2428–2436.

Parrizas M, Maestro MA, Boj SF, Paniagua A, Casamitjana R, Gomis R, Rivera F, Ferrer J. 2001. Hepatic nuclear factor 1-alpha directs nucleosomal hyper-acetylation to its tissue-specific transcriptional targets. Mol Cell Biol 21(9): 3234–3243.

Paul T, Li S, Khurana S, Leleiko NS, Walsh MJ. 2007. The epigenetic signature of CFTR expression is co-ordinated via chromatin acetylation through a complex intronic element. Biochem J 408(3):317–326.

Phillips JE, Corces VG. 2009. CTCF: Master weaver of the genome. Cell 137(7):1194–1211.

Pickersgill H, Kalverda B, de Wit E, Talhout W, Fornerod M, van Steensel B. 2006. Characterization of the Drosophila melanogaster genome at the nuclear lamina. Nat Genet 38(9):1005–1014.

Roh TY, Wei G, Farrell CM, Zhao K. 2007. Genome-wide prediction of conserved and nonconserved enhancers by histone acetylation patterns. Genome Res 17(1):74–81.

Sadoni N, Langer S, Fauth C, Bernardi G, Cremer T, Turner BM, Zink D. 1999. Nuclear organization of mammalian genomes: Polar chromosome territories build up functionally distinct higher order compartments. J Cell Biol 146(6): 1211–1226.

Sadoni N, Targosz BS, Englmann A, Fesser S, Koch J, Schindelhauer D, Zink D. 2008. Transcription-dependent spatial arrangements of CFTR and conserved adjacent loci are not conserved in human and murine nuclei. Chromosoma 117(4):381–397.

Schübeler D, Francastel C, Cimbora DM, Reik A, Martin DIK, Groudine M. 2000. Nuclear localization and histone acetylation: A pathway for chromatin opening and transcriptional activation of the human b-globin locus. Genes Dev 14:940–950.

Smith AN, Barth ML, McDowell TL, Moulin DS, Nuthall HN, Hollingsworth MA, Harris A. 1996. A regulatory element in intron 1 of the cystic fibrosis transmembrane conductance regulator gene. J Biol Chem 271(17):9947–9954.

Somech R, Shaklai S, Geller O, Amariglio N, Simon AJ, Rechavi G, Gal-Yam EN. 2005. The nuclear-envelope protein and transcriptional repressor LAP2-beta interacts with HDAC3 at the nuclear periphery, and induces histone H4 deacetylation. J Cell Sci 118(Pt 17):4017–4025.

Soutoglou E, Viollet B, Vaxillaire M, Yaniv M, Pontoglio M, Talianidis I. 2001. Transcription factor-dependent regulation of CBP and P/CAF histone acetyltransferase activity. EMBO J 20(8):1984–1992.

Splinter E, Heath H, Kooren J, Palstra RJ, Klous P, Grosveld F, Galjart N, de Laat W. 2006. CTCF mediates long-range chromatin looping and local histone modification in the beta-globin locus. Genes Dev 20(17):2349–2354.

Strasak L, Bartova E, Harnicarova A, Galiova G, Krejci J, Kozubek S. 2009. H3K9 acetylation and radial chromatin positioning. J Cell Physiol 220(1): 91–101.

Taimen P, Pfleghaar K, Shimi T, Moller D, Ben-Harush K, Erdos MR, Adam SA, Herrmann H, Medalia O, Collins FS, Goldman AE, Goldman RD. 2009. A progeria mutation reveals functions for lamin A in nuclear assembly, architecture, and chromosome organization. Proc Natl Acad Sci USA 106(49):20788–20793.

Tanabe H, Habermann FA, Solovei I, Cremer M, Cremer T. 2002. Non-random radial arrangements of interphase chromosome territories: Evolutionary considerations and functional implications. Mutat Res 504(1–2):37–45.

Thomas JW, Touchman JW, Blakesley RW, Bouffard GG, Beckstrom-Sternberg SM, Margulies EH, Blanchette M, Siepel AC, Thomas PJ, McDowell JC, Maskeri B, Hansen NF, Schwartz MS, Weber RJ, Kent WJ, Karolchik D, Bruen TC, Bevan R, Cutler DJ, Schwartz S, Elnitski L, Idol JR, Prasad AB, Lee-Lin SQ, Maduro VV, Summers TJ, Portnoy ME, Dietrich NL, Akhter N, Ayele K, Benjamin B, Cariaga K, Brinkley CP, Brooks SY, Granite S, Guan X, Gupta J, Haghighi P, Ho SL, Huang MC, Karlins E, Laric PL, Legaspi R, Lim MJ, Maduro QL, Masiello CA, Mastrian SD, McCloskey JC, Pearson R, Stantripop S, Tiongson EE, Tran JT, Tsurgeon C, Vogt JL, Walker MA, Wetherby KD, Wiggins LS, Young AC, Zhang LH, Osoegawa K, Zhu B, Zhao B, Shu CL, De Jong PJ, Lawrence CE, Smit AF, Chakravarti A, Haussler D, Green P, Miller W, Green ED. 2003. Comparative analyses of multi-species sequences from targeted genomic regions. Nature 424(6950):788–793.

Witcher M, Emerson BM. 2009. Epigenetic silencing of the p16(INK4a) tumor suppressor is associated with loss of CTCF binding and a chromatin boundary. Mol Cell 34(3):271–284.

Yusufzai TM, Tagami H, Nakatani Y, Felsenfeld G. 2004. CTCF tethers an insulator to subnuclear sites, suggesting shared insulator mechanisms across species. Mol Cell 13(2):291–298.

Zenklusen JC, Conti CJ, Green ED. 2001. Mutational and functional analyses reveal that ST7 is a highly conserved tumor-suppressor gene on human chromosome 7q31. Nat Genet 27(4):392–398.

Zhang H, Tasnim F, Ying JY, Zink D. 2009. The impact of extracellular matrix coatings on the performance of human renal cells applied in bioartificial kidneys. Biomaterials 30(15):2899–2911.

Zink D. 2006. The temporal program of DNA replication: New insights into old questions. Chromosoma 115(4):273–287.

Zink D, Amaral MD, Englmann A, Lang S, Clarke LA, Rudolph C, Alt F, Luther K, Braz N, Sadoni N, Rosenecker J, Schindelhauer D. 2004. Transcription-dependent spatial arrangements of CFTR and adjacent genes in human cell nuclei. J Cell Biol 166:815–825.

Zlatanova J, Caiafa P. 2009a. CCCTC-binding factor: To loop or to bridge. Cell Mol Life Sci 66(10):1647–1660.

Zlatanova J, Caiafa P. 2009b. CTCF and its protein partners: Divide and rule? J Cell Sci 122(Pt 9):1275–1284.